

# Incorporating a machine learning technique to improve open-channel flow computations

Hamed Farhadi<sup>1</sup> · Abdolreza Zahiri<sup>2</sup> · M. Reza Hashemi<sup>3</sup> · Kazem Esmaili<sup>1</sup>

Received: 25 May 2016 / Accepted: 17 June 2017  
© The Natural Computing Applications Forum 2017

**Abstract** The objective of this study is to employ support vector machine as a machine learning technique to improve flow discharge predictions in compound open channels. Accurate estimation of channel conveyance is a major step in prediction of the flow discharge in open-channel flow computations (e.g., river flood simulations, design of canals, and water surface profile computation). Common methods to estimate the conveyance are highly simplified and are a main source of uncertainty in compound channels, since popular river/canal models still incorporate 1-D hydrodynamic formulations. Further, the reliability of using a specific method (e.g., vertical divided channel method, the coherence method) over other methods for different applications involving various geometric and hydraulic conditions is questionable. Using available experimental and field data, a novel method was developed, based on SVM, to compute channel conveyance. The data included 394 flow rating curves from 30 different laboratory and natural compound channel sections which were used for the training, and verification of the SVM method. The data were limited to straight compound channels. The performance of SVM was compared with those from other commonly used methods, such as the vertical divided channel method, the coherence method and

the Shiono and Knight model. Additionally, SVM estimations were compared with available data for River Main and River Severn, UK. Results indicated that SVM outperforms traditional methods for both laboratory and field data. It is concluded that the proposed SVM approach could be applied as a reliable technique for the prediction of flow discharge in straight compound channels. The proposed SVM can be potentially incorporated into 1-D river hydrodynamic models in future studies.

**Keywords** Compound channels · Support vector machine · Stage–discharge relationship · Machine learning

## List of symbols

$A$	Cross-sectional area
$b$	Bias term
$C$	Penalty parameter
COH	Coherence parameter
$D(\alpha)$	Dual function
$D_r$	Relative depth (ratio of floodplain depth to main channel depth)
DISADF	Discharge adjustment factor
DISDEF	Discharge deficit
$f$	SVM function
$h$	Bank-full depth
$H$	Flow depth
$K$	Conveyance parameter
$K(x_i, x_j)$	Kernel function
$L$	Lagrange function
$L_\epsilon$	Loss function
MAPE	Mean absolute percentage error
$n$	Manning coefficient
$P$	Wetted perimeter
$Q_b$	Bank-full discharge
$Q_m$	Measured flow discharge

✉ M. Reza Hashemi  
reza\_hashemi@uri.edu

<sup>1</sup> Department of Water Science and Engineering, Ferdowsi University of Mashhad, Mashhad, Iran

<sup>2</sup> Department of Water Engineering, Gorgan University of Agricultural Sciences and Natural Resources, Gorgan, Iran

<sup>3</sup> Department of Ocean Engineering; Graduate School of Oceanography, University of Rhode Island, Narragansett, RI, USA

$Q_p$	Predicted flow discharge
$Q_t$	Total flow discharge
$Q_{VDCM}$	Discharge calculated by VDCM
$r$	Lagrangian multiplier
$R$	Risk function
$R^2$	Coefficient of determination
Residual	Difference between predicted and observed results
RMSE	Root mean square error
SVM	Support vector machine
$s$	Channel side slope
$S_0$	Longitudinal slope
$s_f$	Friction slope
$U_d$	Depth-averaged velocity
$w$	Weight parameter
$x$	Difference of observed data and mean observed data
$X$	Observed data
$\bar{X}$	Mean observed data
$X_i$	Data used to build the SVM model
$X_{max}$	Maximum of data values
$X_{min}$	Minimum of data values
$X_n$	Normalized data
$y$	Difference of predicted data and mean predicted data
$Y$	Predicted data
$\bar{Y}$	Mean predicted data
$y_i$	Target values
$\alpha$	Lagrangian multiplier
$\Gamma$	Secondary flow parameter
$\varepsilon$	Parameter of insensitive loss function
$\lambda$	Dimensionless eddy viscosity
$\xi$	Slack variable
$\psi$	Higher-dimensional space map function

## 1 Introduction

Most natural rivers do not have simple cross section, and have complex or compound geometries (Fig. 1). A compound channel is composed of a main channel and flood plains. The most popular equation used to approximate river and stream's discharge is the Manning equation—in steady, unsteady, uniform and non-uniform conditions. In particular, for a compound channel, the channel cross section is usually divided into main channel and floodplains subsections. This method is based on a geometrical calculation of discharge capacity and is called the divided channel method (DCM). Methods that are based on the geometric division of a channel cross section, are not accurate, because they do not take into account the momentum transfer between the main channel and

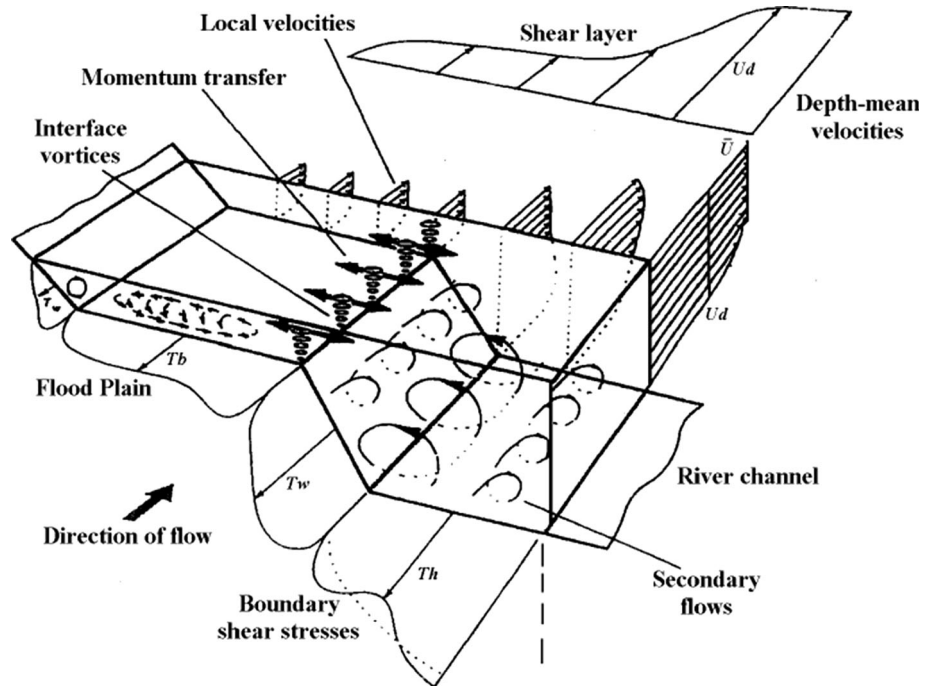
floodplains. Several studies have shown the inaccuracy of geometrical methods for compound channels (e.g., Knight and Hamed [1], Wormleaton and Hadjipanos [2], and Myers and Lyness [3]). Also, Martin and Myers [4] and Lai and Bessaih [5] demonstrated that the maximum error of using vertical divided channel method (VDCM) in river and flume compound channels may be up to 40 and 60%, respectively. To address this issue, some researchers have proposed alternative empirical equations and analytical methods to compute discharge capacity in straight compound channels. Among these methods, the coherence method (COHM) of Ackers [6, 7] and the Shiono and Knight Model (SKM) [8, 9] are more popular [10, 11], as they improve the results significantly considering their assumptions. However, these methods involve considerable computational effort and, in general, cannot be conveniently applied [12].

In recent years, several data-driven methods have been proposed to find the relationship between the flow discharge and hydraulic and geometric properties of compound channels: artificial neural networks [11, 13–15], genetic algorithm [10, 16], linear genetic programming [17] and M5 tree decision models [12]. Data-driven methods attempt to correlate the variables, usually inputs and outputs, using any mathematical expression and regardless of the physical processes involved—and therefore avoid uncertainties which are associated with understanding these processes. Data-driven methods may lead to more accurate results, using less computational effort, but their application is usually limited to training data.

Support vector machine (SVM) is a machine learning method, which has attracted much interest in various fields of earth science, and has led to encouraging results in hydrology and water resources research. Some applications of SVM include rainfall–runoff modeling [18, 19], evapotranspiration predictions [20–22], flood forecasting [23–26] and groundwater modeling [27–30]. SVM has attractive properties; for instance, it delivers a unique solution, since its optimization methodology is convex. This is an advantage compared to other machine learning methods, which have multiple solutions associated with local minima and may not be robust over different samples [31]. In addition, SVM uses kernel functions as a trick to model nonlinear relations.

Here, we examined the performance of SVM in predicting flow discharge in straight compound channels. A brief description of momentum transfer in compound channels, and a review of methods used for conveyance estimation are given in the next section. Then, a description of datasets used for training and verification of the SVM is provided. SVM results for prediction of discharge in laboratory and natural channels are discussed in Sect. 3. Some conclusions are presented at the end.

**Fig. 1** Flow structure in a compound channel (after Shiono and Knight [9])



## 2 Methods

### 2.1 Momentum transfer in compound channels

A compound channel consists of a main channel and flood-plain/s on one or both sides. Since in non-flood events, flow is generally limited to the main channel, the bed roughness is lower than the floodplains which are almost dry or vegetated. Floodplains are usually much wider than the main channel. Therefore, during a flooding event that leads to inundation, the flow velocity in the main channel is considerably larger than those in the floodplains. This difference causes momentum transfer between the main channel and floodplains. The momentum transfer leads to a significant reduction in the total discharge capacity of a channel (Fig. 1).

### 2.2 The vertical divided channel method (VDCM)

To apply this method, a typical prismatic compound channel with three subdivided sections which are separated by vertical lines is shown in Fig. 2. The sum of discharges

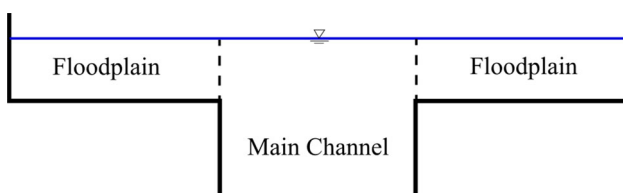


**Fig. 2** Schematic division of a compound channel by a vertical section method

that are calculated in each subsection by the Manning equation is the total flow discharge [32]:

$$Q_{VDCM} = \sum_{i=1}^N Q_i = \sum_{i=1}^N \frac{A_i R_i^{2/3} S_0^{1/2}}{n_i} \quad (1)$$

where  $Q_{VDCM}$  is total flow discharge in compound channel,  $A$ ,  $R$ ,  $S_0$  and  $n$  are area, hydraulic radius, bed slope and the Manning coefficient, respectively.  $N$  is the total number of subsections (2 or 3 corresponding to the main channel and floodplains). The vertical divided channel method is a common technique in engineering tools and hydraulic models. As mentioned before, this method may lead to a significant overestimation error for discharge estimations in compound sections [6].

### 2.3 Coherence method

Considering the interaction between the main channel and floodplains, Ackers [6, 7] modified the flow discharge prediction procedure for compound channels. He defined the coherence parameter as the ratio of the basic discharge calculated by treating the channel as a single unit to that calculated by the vertical divided channel method. The coherence (COH) parameter is defined in the form of Eq. 2,

$$COH = \frac{A^{5/3} / (\sum_{i=1}^N n_i^{1.5} p_i)^{2/3}}{\sum_{i=1}^N \frac{1}{n_i} \frac{A_i^{5/3}}{p_i^{2/3}}} \quad (2)$$

where  $p_i$  and  $A_i$  are the wetted perimeter and the area of subsections, respectively.  $P$  and  $A$  are total wetted

perimeter and area of the channel. Alternatively, Eq. (3) can be used more conveniently to compute COH,

$$COH = \frac{(1 + A^*)^{3/2} / \sqrt{\left(1 + \frac{P^{*4} n^{*2}}{A^{*3}}\right)}}{1 + A^{*5/3} / n^* P^{*2/3}} \quad (3)$$

The star (\*) symbol represents the ratio of a parameter value in the floodplain to that in the main channel. A COH close to 1 indicated that a compound channel can be accurately treated as a simple channel. As COH deviated from 1, this approximation leads to errors. By analyzing the smooth compound channel data of flood channel facility (FCF), Ackers [6, 7] suggested different degrees of interference between the main channel and floodplain flow according to the relative depth (ratio of water depth in floodplain to that in main channel). After plotting the discharge adjustment factor (DISDAF), which is the ratio of actual discharge to summation of zonal calculated discharges by vertical approach, against relative depth, four distinct regions with different trends could be recognized (Fig. 3).

In region 1, the relative depth is low. Therefore, the interaction between the main channel and floodplains increases with depth, up to the relative depth of 0.2. Region 2 is related to the relative depths between 0.2 and 0.4, where the interaction effect decreases. In region 3, flow depth is getting further higher and presumably because of some changes in secondary currents, the interaction effect increases up to the relative depth of 0.5 [7]. In region 4, the interaction between the main channel and floodplains is low enough to treat the channel as a single unit. The equations of Ackers' method to estimate discharge in compound channels are provided in Table 1.

**Fig. 3** Discharge adjustment factor (DISDAF) against relative depth for FCF test series 2 (after Ackers [7])

### 2.4 Shiono and Knight model (SKM)

Shiono and Knight [8, 9] presented their quasi-2D model, which is based on Reynolds-averaged Navier–Stokes (RANS) equations, for a steady uniform flow in a channel as follows,

$$\begin{aligned} \rho g H S_0 - \rho \frac{f}{8} U_d^2 \sqrt{1 + \frac{1}{s^2}} + \frac{\partial}{\partial y} \left[ \rho \lambda H^2 \sqrt{\frac{f}{8}} U_d \frac{\partial U_d}{\partial y} \right] \\ = \frac{\partial}{\partial y} [H(\rho UV)_d] \end{aligned} \quad (4)$$

where  $\rho$  is the water density,  $g$  is the gravitational acceleration,  $f$  is the friction factor,  $H$  is local depth flow,  $y$  denotes the transverse direction with the origin at the side wall,  $U_d$  is the depth-averaged stream-wise velocity,  $s$  is the side slope of the channel,  $\lambda$  is the dimensionless eddy viscosity,  $V$  is the lateral, and  $U$  is the longitudinal mean velocity. The right hand side of Eq. 4 accommodates the effect of secondary current, which for mathematical convenience will be represented by  $\Gamma$ . In this paper, conveyance estimation system (CES) software [33], which is based on the Shiono and Knight model [9], is used to calculate the flow capacity in all studied channels. CES considers  $\lambda = 0.24$  for main channel ( $\lambda_{mc}$ ) as default; however, it can be changed by user, while  $\lambda$  for a floodplain ( $\lambda_{fp}$ ) is calculated by the following equation as recommended by Abril and Knight [34]:

$$\lambda_{fp} = \lambda_{mc} (-0.2 + 1.2 D_r^{-1.44}) \quad (5)$$

where  $D_r$  is the ratio of floodplain depth to main channel depth. The secondary flow term ( $\Gamma$ ) can be calculated

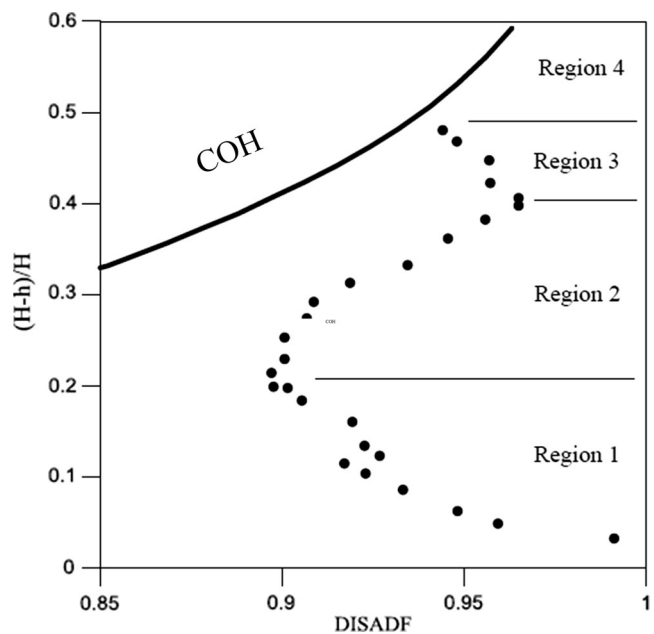


**Table 1** Summary of equations involved in calculation of discharge by COH method

Region	Equation	DISDEF	DISADF
1	$Q = Q_{VDCM} - DISDEF$	$(Q_{2c}^* + N_f Q_{2f}^*)(V_c - V_f)Hh \times ARF$	
2	$Q = Q_{VDCM} \times DISADF_2$		COH( $[D_r + \text{shift}]$ )
3	$Q = Q_{VDCM} \times DISADF_3$		1.567 - 0.667 COH
4	$Q = Q_{VDCM} \times DISADF_4$		COH

Regions have been shown in Fig. 3

$Q_{2c}^*$ ,  $V_c$ ,  $Q_{2f}^*$  and  $V_f$  are discharge deficit and velocity in the main channel and floodplain, respectively.  $H$  and  $h$  are flow depths in the main channel and floodplain, respectively. ARF is aspect ratio factor. In region 2, a shift in relative depth is needed to estimate discharge more accurate, which is 0.15 for main channel side slope  $s_c \geq 1$  [7]

depending on the water level in the channel (inbank, overbank, flood plain scenarios) which is recommended by Abril and Knight [34] as follows:

$$\Gamma_{mci} = 0.05H\rho gS_0 \tag{6}$$

$$\Gamma_{mco} = 0.15H\rho gS_0 \tag{7}$$

$$\Gamma_{fp} = -0.25H\rho gS_0 \tag{8}$$

where  $\Gamma_{mci}$ ,  $\Gamma_{mco}$  and  $\Gamma_{fp}$  are secondary current parameters for main channel inbank, overbank and floodplain scenarios, respectively.

### 2.5 Support vector machines

Support vector machine (SVM) is a learning machine method developed by Vapnik and his colleagues [35, 36]. Initial applications of support vector machine included classification and pattern recognition [37]. Excellent performance of SVM was reported in regression and time-series analysis applications [38]. The basic idea of SVM is to map the training data from the input space to a higher-dimensional feature space via a kernel function  $\phi$  and then to construct a hyperplane with maximum margin in the feature space. Therefore, SVM uses linear functions in a higher-dimensional space to classify linearly, for classification purposes and interpolate a set of training data linearly, for regression purposes. In this study, the  $\epsilon$ -SVM method [39] was used to construct an input–output model. Considering a set of training data as  $\{(x_1, y_1), (x_2, y_2), \dots, (x_l, y_l)\} \subset \chi \times R$ , where  $\chi$  denotes the space of input patterns. The linear function in space of  $x$  could be described as follows,

$$f(x) = w \cdot x + b \tag{9}$$

where  $w$  is the weight and  $b$  is the bias term, which are estimated by minimizing the following risk function,

$$R = C \frac{1}{l} \sum_{i=1}^l L_\epsilon(y_i, f_i) + \frac{1}{2} \|w\|^2 \tag{10}$$

where  $C$  is constant called penalty and  $L_\epsilon$  is loss function described in Eq. (11),  $y_i$  and  $f_i$  are actual target values and estimated target values by Eq. (9), respectively.

$$L_\epsilon(y_i, f_i) = \begin{cases} 0 & \text{if } |y_i - f_i| \leq \epsilon \\ |y_i - f_i| - \epsilon & \text{otherwise} \end{cases} \tag{11}$$

The goal is to find  $f(x)$  which has at most  $\epsilon$  deviation from the actually obtained targets  $y_i$  for all the training data, and at the same time as flat as possible [39]. This can be visualized as a band or a tube around the separable hyperplane with points outside of the band considered as training errors (Fig. 4). Therefore, in addition to finding an optimum  $f(x)$  by considering flatness (function curvature) training errors (i.e., slack variables) should be minimized. Thus, the optimization problem becomes,

$$\text{minimize} \left( \frac{1}{2} \|w\|^2 + C \sum_{i=1}^n (\xi_i + \xi_i^*) \right) \tag{12}$$

Subjected to the following constraints,

$$\begin{aligned} y_i - (w \cdot x) - b &\leq \epsilon + \xi_i \\ (w \cdot x) + b - y_i &\leq \epsilon + \xi_i^* \\ \xi_i, \xi_i^* &\geq 0 \end{aligned}$$

To solve this optimization problem, quadratic programming (QP) method can be used. First, the Lagrange

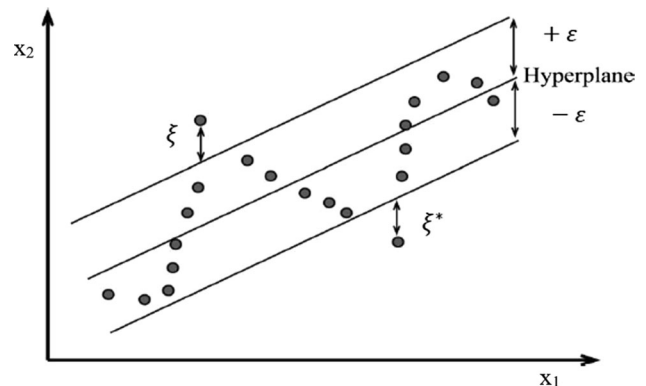


**Fig. 4** Schematic positive and negative slack variables

function, which contains target function with its subjects, is formed.

$$L = \frac{1}{2} \|w\|^2 + C \sum_{i=1}^n (\zeta_i + \zeta_i^*) - \sum_{i=1}^n \alpha_i [(w_i \cdot x + b) - y_i + (\varepsilon + \zeta_i)] - \sum_{i=1}^n \alpha_i^* [y_i - (w_i \cdot x + b) + (\varepsilon + \zeta_i^*)] - \sum_{i=1}^n [r_i \zeta_i + r_i^* \zeta_i^*] \tag{13}$$

where  $\alpha_i$ ,  $\alpha_i^*$ ,  $r_i$  and  $r_i^*$  are Lagrange multipliers and for any data they are nonnegative. Equation (13) is minimized with respect to variables  $w$ ,  $b$ ,  $\zeta$  and  $\zeta^*$  and is maximized with respect to Lagrange multipliers  $\alpha$ ,  $\alpha^*$ ,  $r$  and  $r^*$ . After differentiating with respect to these parameters and setting the derivatives to zero, Eqs. (14)–(17) are obtained.

$$\frac{\partial L}{\partial w} = 0 \rightarrow w = \sum_{i=1}^N (\alpha_i - \alpha_i^*) x_i \tag{14}$$

$$\frac{\partial L}{\partial b} = 0 \rightarrow \sum_{i=1}^N (\alpha_i - \alpha_i^*) = 0 \tag{15}$$

$$\frac{\partial L}{\partial \zeta_i} = 0 \rightarrow C = \alpha_i + r_i \tag{16}$$

$$\frac{\partial L}{\partial \zeta_i^*} = 0 \rightarrow C = \alpha_i^* + r_i^* \tag{17}$$

By substituting these equations into Eq. (13), a dual Lagrangian function dependent only on  $\alpha$  is obtained, which requires to be maximized.

$$\max(D(\alpha)) = \max \left( \sum (\alpha_i - \alpha_i^*) y_i - \varepsilon \sum (\alpha_i - \alpha_i^*) - \frac{1}{2} \sum_{i=1}^N \sum_{j=1}^N (\alpha_i - \alpha_i^*) (\alpha_j - \alpha_j^*) K(x_i, x_j) \right) \tag{18}$$

subjected to the following constraints,

$$\sum (\alpha_i - \alpha_i^*) = 0 \quad 0 \leq \alpha_i \leq C \quad 0 \leq \alpha_i^* \leq C$$

where  $K(x_i, x_j)$  is the kernel function.

Kernel function is a method to handle input spaces, which are not linear in the space of  $x$ , but can linearly be regressed in a higher-dimensional space of  $\psi(x)$ . Therefore, the kernel function job is to map  $x$  to  $\psi(x)$ . In order to use the kernel method, in previous equations,  $\psi(x)$  substitutes for  $x$ . The kernel function is,

$$K(x_i, x_j) = \psi(x_i) \cdot \psi(x_j) \tag{19}$$

The SVM regression function modeling the data after modifying Eq. (9) by considering Eqs. (18) and (19) can be written as follows,

$$f = \sum_{i=1}^N (\alpha_i - \alpha_i^*) K(x_i, x_j) + b \tag{20}$$

### 2.6 SVM model structure

In this study, radial basis function ( $\exp(-\gamma \|x_i - x_j\|^2)$ ) was used as the kernel function to map data into a feature space, which makes it possible to use linear regression. Hence, three parameters need to be selected in a way to reach an optimum solution.  $C$  and  $\varepsilon$  are SVM model parameters, and  $\gamma$  is the RBF parameter. These parameters were determined by grid search technique for the best results, and they include  $\gamma = 2.7$ ,  $C = 5$  and  $\varepsilon = 0.0151$ . Contour map of grid search result for verification phase according to RMSE criterion is shown in Fig. 5.

In this study, LIBSVM [40] was used as a tool to implement SVM model in MATLAB. A general flowchart of SVM regression structure which is used to model the input–output is shown in Fig. 6.

### 2.7 Data preparation

In this research, 394 flow rating curves data from 30 different straight compound sections were used from experimental flumes and natural rivers. Several experimental datasets were combined for the analysis including HR Wallingford dataset for compound channel flumes [41], data from Blalock and Sturm [42], Knight and Demetriou [43], Lambert and Sellin [44], Martin and Myers [4], Lambert and Myers [45], Bousmar and Zech [46], Haidera and Valentine [47], Lai and Bessaih [5] and Bousmar et al. [48]. Additionally, field data were used from rivers, including River Severn at Montford Bridge [6, 49], River Main [4] and Colorado River [50]. The ratio of the flume data to natural rivers data was about 80–20%. The cross section of an idealized river compound channel is shown in Fig. 7. The ranges of geometric and hydraulic characteristics of compound channels used in this study are listed in Table 2. The dataset was divided into a training set (70% of data) and a verification set (30%). The training and the verification data were randomly selected. Then, these subsets were checked to make sure they have similar statistical parameters (mean and standard deviation) in order to be statistically representative of the entire dataset. The random selection was repeated in case that statistical parameters were significantly different for the training and the verification data. In order to do this, two null hypothesis were performed by  $t$  test, for no significant difference between means of two samples (verification and training subsets), and F test for no significant difference between standard deviation of two samples. Data division was

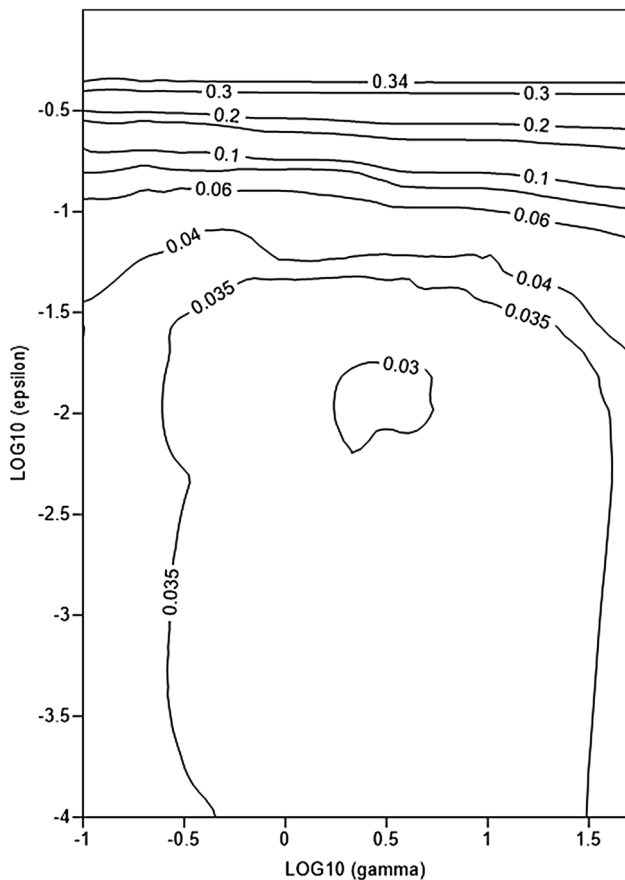


**Fig. 5** Contour map of the grid search result for  $C = 5$ ; the contours show dimensionless error

performed in a way that these hypotheses would be accepted in a significance level of 0.05.

Since a wide range of data with different scales were used, with the application of Eq. (21), input data are first normalized to a range between 0 and 1. The normalization helps to speed up the model convergence. The data are normalized using the following equation,

$$X_n = \frac{X_i - X_{\min}}{X_{\max} - X_{\min}} \quad (21)$$

where  $X_n$  is the normalized data,  $X_i$  is the raw data, and  $X_{\min}$  and  $X_{\max}$  are the minimum and maximum of data.

In this paper, it is assumed (similar to Ackers [6, 7] approach) that discharge ratio in compound open channels is dependent on three input dimensionless parameters, including relative depth,  $D_r$ , coherence parameter, COH, and calculated discharge ratio ( $\frac{Q_{VDCM}}{Q_b}$ ).

$$\frac{Q_t}{Q_b} = f\left(D_r, COH, \frac{Q_{VDCM}}{Q_b}\right) \quad (22)$$

where  $Q_t$  and  $Q_b$  are total and bank-full flow discharges, respectively.

## 2.8 Statistical evaluation of performance

To validate the results of the training and verification phases, several common statistics were used:  $R^2$  (coefficient of determination), RMSE (root mean square error), MAPE (mean absolute percentage error), and residual. They are defined as follows:

$$R^2 = \left(\frac{\sum xy}{\sqrt{\sum x^2 \sum y^2}}\right)^2 \quad (23)$$

$$RMSE = \sqrt{\frac{\sum (X - Y)^2}{n}} \quad (24)$$

$$MAPE = \frac{100}{n} \sum \frac{|X - Y|}{X} \quad (25)$$

$$Residual = Q_p - Q_t \quad (26)$$

where  $x = X - \bar{X}$ ,  $y = Y - \bar{Y}$ ,  $X$  is the observed data,  $Y$  is the predicted data,  $\bar{X}$ ,  $\bar{Y}$ ,  $Q_p$  and  $Q_t$  are the mean observed data, mean predicted data, predicted discharge and measured discharge, respectively.  $n$  is the number of data.

## 3 Results and discussion

The performance of the proposed SVM model was evaluated by the statistical parameters introduced in the previous section. Some commonly used methods such as VDCM, COHM and SKM along with observed data were used for comparison. Figure 8 shows the performance of SVM and other methods against observed data for training, verification and all data. In Fig. 8, the first, second and third columns correspond to the training, verification, and all data cases. Referring to Fig. 8, it can be seen that SVM outperforms other methods in prediction of discharge ratio for all phases. Table 3 shows a quantitative evaluation of the performance of each method. Considering verification phase, SVM provided the smallest RMSE ( $0.030 \text{ m}^3/\text{s}$ ) and MAPE (6.65) and the highest  $R^2$  (0.97), in comparison with other methods. To assess the relative importance of input variables on prediction results, a sensitivity analysis was carried out. As shown in Table 4, various combinations of input variables were considered and their influence on results was evaluated in terms of  $R^2$  and RMSE. This table indicates that  $D_r$  and COH have less effect on the results compared to  $\frac{Q_{VDCM}}{Q_t}$ . This table also shows  $D_r$  and COH lead to better results when they are used together rather than separately. However, as  $D_r$  and COH are important hydraulic parameters which include flow and geometrical properties of channels, also considering the uncertainty of data, we recommend using all of the input variables. To further assess the skill of the model, the

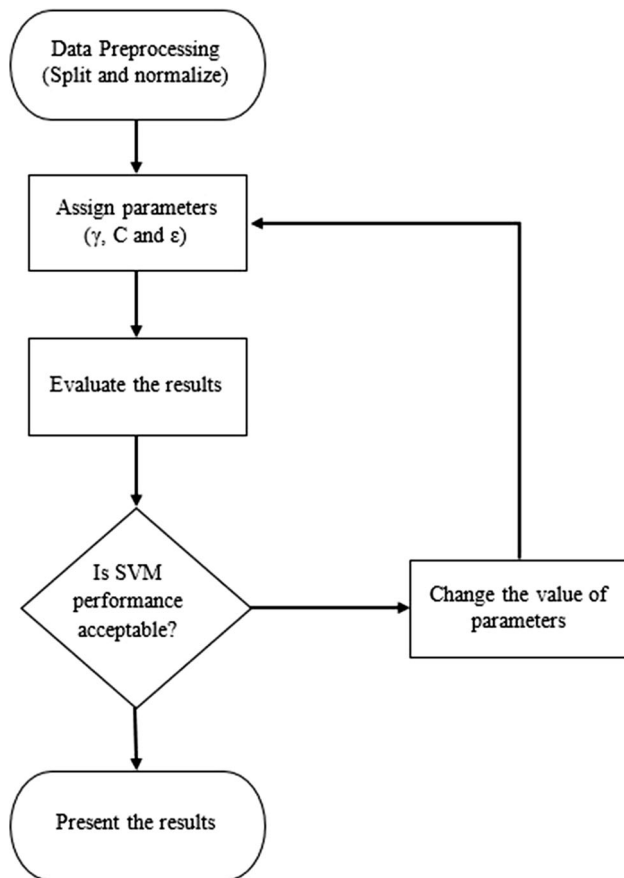


**Fig. 6** Flowchart of SVM regression algorithm for modeling the discharge in straight compound channels

**Fig. 7** A typical river compound cross section

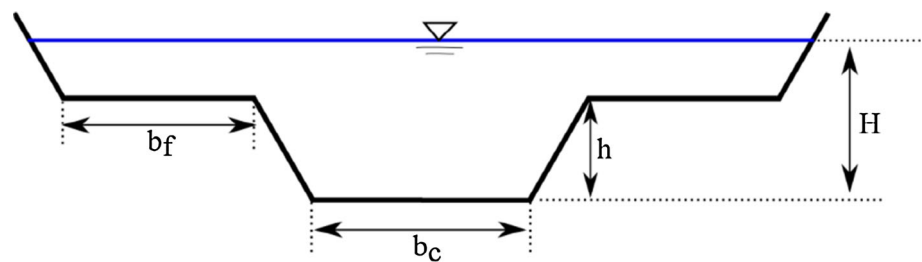


**Table 2** Range of geometric and hydraulic variables of compound channels

Symbol	Variable definition	Variable range	Mean value
$h(m)$	Bank-full height	0.031–6	0.811
$b_c(m)$	Main channel width	0.152–21.4	3.2
$b_f(m)$	Floodplain width	0–63	6.5
$n_c$	Manning roughness coefficient of main channel	0.01–0.036	0.0133
$n_f$	Manning roughness coefficient of floodplain	0.01–0.05	0.0166
$s_0$	Bed slope	0.000185–0.005	0.0011
$H(m)$	Flow depth	0.036–7.81	0.985
$Q_b(m^3/s)$	Bank-full discharge	0.00268–172.048	20.99
$Q_t(m^3/s)$	Total flow discharge	0.003–560	30.486

observed data of two different types of cross sections including laboratory channels (FCF) and natural channels (River Main and River Severn) were also considered in the analysis. For this analysis, smooth type of FCF compound channels with a height of 0.15 m for the main channel, the Manning roughness coefficient of 0.01 and the average longitudinal slope of 0.001027 for all cross sections was considered. For River Main, an upstream section which is approximately straight was considered. The bed material in main channel of river is coarse gravel with a  $d_{50}$  of 10–20 mm, while the main channel banks consist of boulders up to 1 m in diameter and the floodplains are covered with grass. The average longitudinal slope is 0.003 [4]. Additionally, a compound channel in River Severn at Montford Bridge, which is a hydrometric station, was examined. The bed material is sand with roughness coefficient of 0.02, and the bank and floodplains are covered with grass and turf, respectively. The average longitudinal slope is chosen 0.000195 for calculation purposes [49].

SVM was applied to these cross sections, and the results are shown in Figs. 8 and 9. SVM outperforms other methods by producing the lowest residuals. Considering Fig. 10, SVM produces lower residuals in all discharges for River Main, and in larger discharges for River Severn. As can be seen from results corresponding to River Severn in Fig. 10, VDCM and COHM discharge estimations are unreliable, whereas SKM performs better. SVM results are convincing, and this technique outperforms the other methods. In addition, average residuals, which were produced by these methods, and the

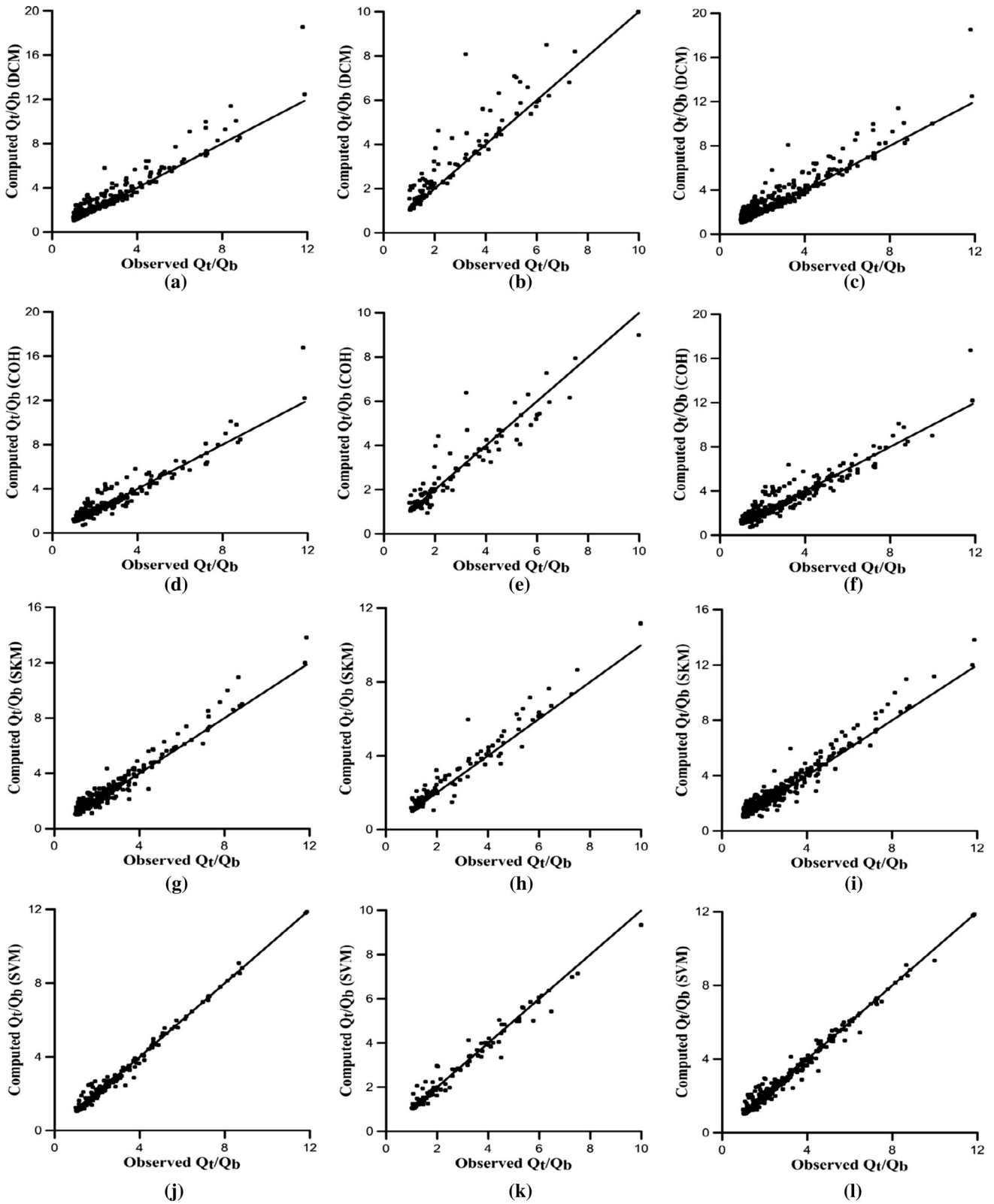


**Fig. 8** Results of comparison between predicted and observed values of discharge ratio ( $Q_t/Q_b$ ) for training phase (column 1), validation phase (column 2) and all data (column 3) by VDCM (a–c), COH (d–f), SKM (g–i) and SVM (j–l)

**Table 3** Prediction results of SVM, VDCM, COHM and SKM

Method	Training phase			Verification phase			All data		
	$R^2$	RMSE <sup>#</sup>	MAPE	$R^2$	RMSE <sup>#</sup>	MAPE	$R^2$	RMSE <sup>#</sup>	MAPE
SVM	0.98	0.023	7.13	0.97	0.030	6.65	0.98	0.025	8.2
VDCM	0.91	0.780	19.00	0.87	0.805	20.04	0.90	0.788	19.31
COHM	0.92	0.580	13.30	0.89	0.587	14.15	0.91	0.582	13.44
SKM	0.95	0.477	13.57	0.94	0.533	14.55	0.95	0.495	13.87

<sup>#</sup> Units, m<sup>3</sup>/s

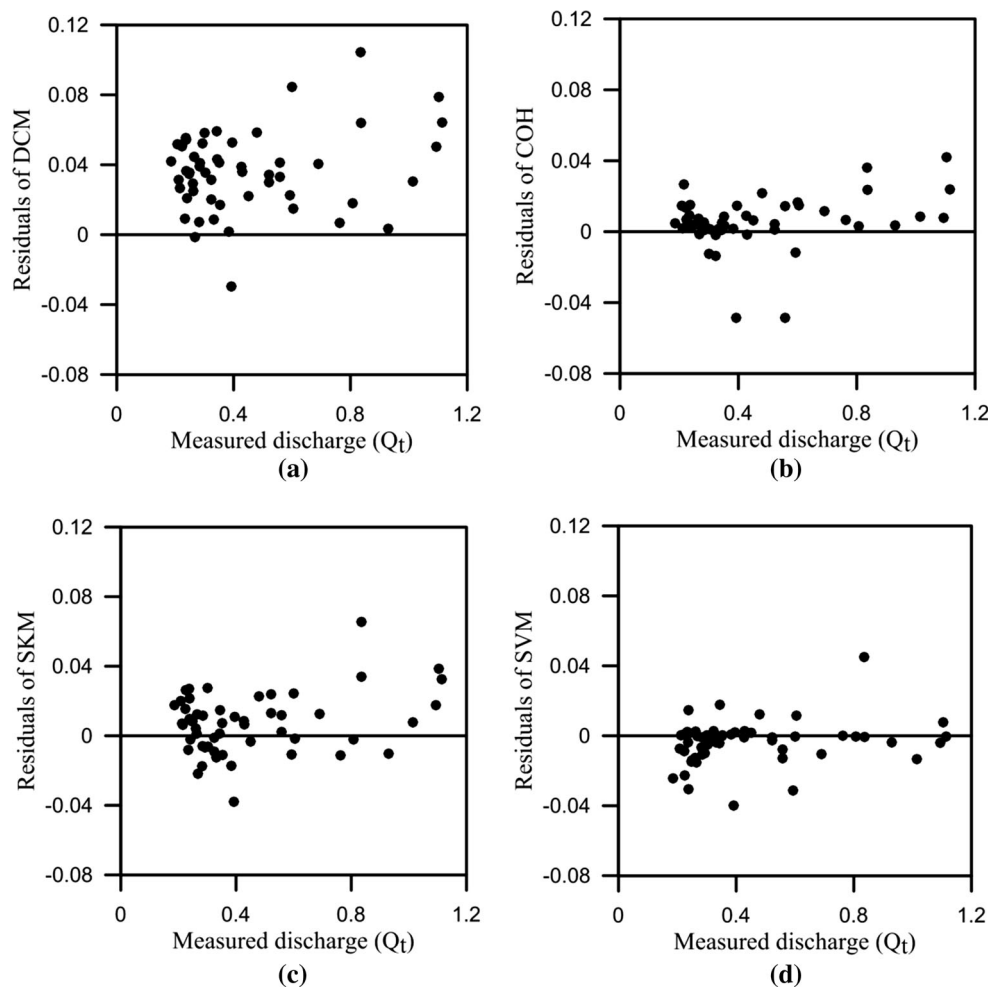
ranking based on better performance are shown in Table 5. Overall, SVM shows a very good performance.

As SVM performance is dependent on the training data, its accuracy can be improved by addition of more datasets. Furthermore, this study was focused on straight channels and, as a result, more research is necessary to apply SVM in meandering channels. Considering the results of this study, VDCM leads to significant errors. Also, COHM needs time-consuming computations. SKM and SVM are recommended for flow discharge predictions in straight compound channels.

**Table 4** Sensitivity analysis of SVM model input variables

No	Input variable/s	$R^2$	RMSE (m <sup>3</sup> /s)
1	$D_r$ , COH	0.92	0.054
2	$D_r$ , $\frac{Q_{VDCM}}{Q_t}$	0.93	0.047
3	COH, $\frac{Q_{VDCM}}{Q_t}$	0.96	0.032
4	$D_r$	0.64	0.105
5	COH	0.52	0.126
6	$\frac{Q_{VDCM}}{Q_t}$	0.91	0.052

**Fig. 9** Residual values against measured discharge of FCF phase-A laboratory data for VDCM (a), COHM (b), SKM (c) and SVM method (d); the unit of residual and discharge is m<sup>3</sup>/s



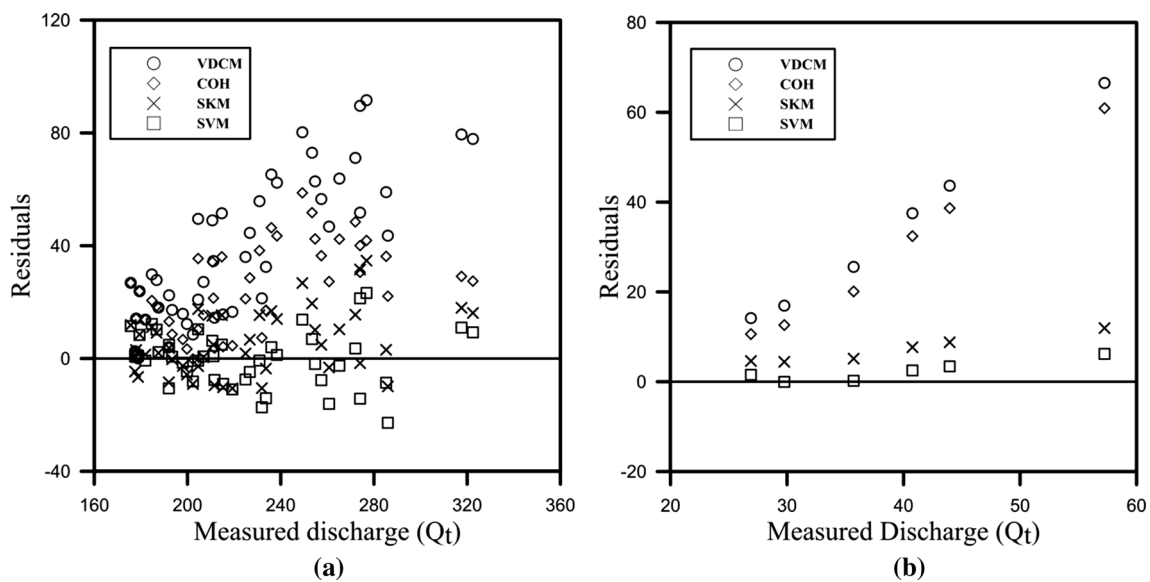


**Fig. 10** Residual values against measured discharge of **a** River Severn at Montford bridge and **b** upstream section of River Main, for VDCM, COHM, SKM and SVM methods; the unit of residual and discharge is  $m^3/s$

**Table 5** Average residuals obtained using VDCM, COHM, SKM and SVM methods

Section	Average residuals ( $m^3/s$ ) of				Rank of method			
	Method							
	VDCM	COHM	SKM	SVM	VDCM	COHM	SKM	SVM
FCF data	0.036	0.005	0.007	-0.004	4	2	3	1
River Main	34.06	29.22	7.10	2.30	4	3	2	1
River Severn	39.57	23.93	5.56	-0.05	4	3	2	1

Another discussion point is the application of this method in dynamic flow routing. Saint–Venant equations are traditionally used to model non-uniform/unsteady flow in rivers and channels. They consist of continuity and momentum equations [32], which are averaged over a cross-sectional area. In particular, the friction slope  $s_f$  in the momentum equation is approximated by Manning equation  $s_f = (\frac{Q}{K})^2$ , where  $K = \frac{1}{n}AR^{2/3}$  is the conveyance term. In other words, the uniform flow assumption is made for friction force estimation in the Saint–Venant equations. In computer models like HEC-RAS, the conveyance term is calculated by summation of all subdivided conveyances in a compound channel [51]. Therefore, same sources of uncertainty may lead to error in the case of compound channels. SVM can theoretically replace this procedure for computation of the conveyance in those models; however, this application needs further research.

### 4 Conclusions

A support vector machine (SVM) method was developed based on available experimental flumes and natural river data to predict flow discharge in straight compound channels. The proposed model uses RBF kernel function and has three dimensionless input parameters including relative depth ( $D_r$ ), coherence (COH) and total computed flow discharge to bank-full discharge ( $\frac{Q_{VDCM}}{Q_b}$ ). SVM performance was compared with those from common methods such as VDCM, COHM and SKM, which represent geometrical, empirical and quasi-2D approaches, respectively. Average performance of SVM for training phase, verification phase and all data is very encouraging, with coefficient of determination  $R^2 = 0.98$ , root mean square error  $RMSE = 0.026 m^3/s$  and mean absolute percentage error  $MAPE = 7.33$ . SVM results were also examined at a

number of cross sections in River Main and River Severn. SVM outperforms other methods in predicting flow discharge with average residual of  $-0.004$ ,  $2.30$  and  $-0.05$  for FCF flumes, River Main and River Severn, respectively. SVM's satisfactory results indicated that it can be applied as a reliable technique for the prediction of flow discharge in straight compound channels. The method can be incorporated into numerical river models with further research.

#### Compliance with ethical standards

**Conflict of interest** The authors declare that they have no conflict of interest.

#### References

1. Knight DW, Hamed ME (1984) Boundary shear in symmetrical compound channels. *J Hydraul Eng* 110(10):1412–1430
2. Wormleaton PR, Hadjipanos P (1985) Flow distribution in compound channels. *J Hydraul Eng* 111(2):357–361
3. Myers R, Lyness J (1997) Discharge ratios in smooth and rough compound channels. *J Hydraul Eng* 123(3):182–188
4. Martin L, Myers W (1991) Measurement of overbank flow in a compound river channel. *ICE Proc* 91(4):645–657
5. Lai S, Bessaih N (2004) Flow in compound channels. In: 1st International conference on managing rivers in the 21st century, Malaysia, pp 275–280
6. Ackers P (1992) Hydraulic design of two-stage channels. *Proc ICE-Water Marit Energy* 96(4):247–257
7. Ackers P (1993) Flow formulae for straight two-stage channels. *J Hydraul Res* 31(4):509–531
8. Shiono K, Knight D (1988) Two-dimensional analytical solution for a compound channel. In: Proceedings of 3rd international symposium on refined flow modelling and turbulence measurements, pp 503–510
9. Shiono K, Knight DW (1991) Turbulent open-channel flows with variable depth across the channel. *J Fluid Mech* 222:617–646
10. Sharifi S, Sterling M, Knight DW (2009) A novel application of a multi-objective evolutionary algorithm in open channel flow modelling. *J Hydroinform* 11(1):31. doi:10.2166/hydro.2009.033
11. Unal B, Mamak M, Seckin G, Cobaner M (2010) Comparison of an ANN approach with 1-D and 2-D methods for estimating discharge capacity of straight compound channels. *Adv Eng Softw* 41(2):120–129. doi:10.1016/j.advengsoft.2009.10.002
12. Zahiri A, Azamathulla HM (2012) Comparison between linear genetic programming and M5 tree models to predict flow discharge in compound channels. *Neural Comput Appl* 24(2):413–420. doi:10.1007/s00521-012-1247-0
13. MacLeod AB (1997) Development of methods to predict the discharge capacity in model and prototype meandering compound channels. University of Glasgow
14. Liu W, James C (2000) Estimation of discharge capacity in meandering compound channels using artificial neural networks. *Can J Civ Eng* 27(2):297–308
15. Zahiri A, Dehghani A (2009) Flow discharge determination in straight compound channels using ANN. *World Acad Sci Eng Technol* 58:1–8
16. Sharifi S (2009) Application of evolutionary computation to open channel flow modelling. University of Birmingham, Birmingham, UK
17. Azamathulla HM, Zahiri A (2012) Flow discharge prediction in compound channels using linear genetic programming. *J Hydrol* 454–455:203–207
18. Dibike YB, Velickov S, Solomatine D, Abbott MB (2001) Model induction with support vector machines: introduction and applications. *J Comput Civ Eng*
19. Bray M, Han D (2004) Identification of support vector machines for runoff modelling. *J Hydroinform* 6:265–280
20. Eslamian S, Gohari S, Biabanaki M, Malekian R (2008) Estimation of monthly pan evaporation using artificial neural networks and support vector machines. *J Appl Sci* 8(19):3497–3502
21. Samui P (2011) Application of least square support vector machine (LSSVM) for determination of evaporation losses in reservoirs. *Engineering* 3(04):431
22. Tabari H, Kisi O, Ezani A, Talaee PH (2012) SVM, ANFIS, regression and climate based models for reference evapotranspiration modeling using limited climatic data in a semi-arid highland environment. *J Hydrol* 444:78–89
23. Han D, Chan L, Zhu N (2007) Flood forecasting using support vector machines. *J Hydroinform* 9(4):267–276
24. Chen S-T, Yu P-S (2007) Pruning of support vector networks on flood forecasting. *J Hydrol* 347(1):67–78
25. Yu P-S, Chen S-T, Chang I-F (2006) Support vector regression for real-time flood stage forecasting. *J Hydrol* 328(3):704–716
26. Hashemi MR, Spaulding ML, Shaw A, Farhadi H, Lewis M (2016) An efficient artificial intelligence model for prediction of tropical storm surge. *Nat Hazards* 82(1):471–491
27. Behzad M, Asghari K, Coppola EA Jr (2009) Comparative study of SVMs and ANNs in aquifer water level prediction. *J Comput Civ Eng* 24(5):408–413
28. Yoon H, Jun S-C, Hyun Y, Bae G-O, Lee K-K (2011) A comparative study of artificial neural networks and support vector machines for predicting groundwater levels in a coastal aquifer. *J Hydrol* 396(1):128–138
29. Liu J, Chang J-X, Zhang W-G (2009) Groundwater level dynamic prediction based on chaos optimization and support vector machine. In: Genetic and evolutionary computing, 2009. WGECC'09. 3rd International Conference on. IEEE, pp 39–43
30. Liu J, Chang M, Ma X (2009) Groundwater quality assessment based on support vector machine. In: HAIHE river basin research and planning approach-proceedings of 2009 international symposium of HAIHE basin integrated water and environment management, pp 173–178
31. Auria L, Moro RA (2008) Support vector machines (SVM) as a technique for solvency analysis. German Institute for Economic Research, Berlin, Germany
32. Chow VT (1959) Open-channel hydraulic. McGraw-Hill, New York
33. McGahey C, Samuels P (2003) Methodology for conveyance estimation in two-stage straight, skewed and meandering channels. In: Proceedings of the XXX congress of the international association for hydraulic research, pp 33–40
34. Abril J, Knight D (2004) Stage-discharge prediction for rivers in flood applying a depth-averaged model. *J Hydraul Res* 42(6):616–629
35. Vapnik V (1995) The nature of statistical learning theory. Springer, Berlin
36. Cortes C, Vapnik V (1995) Support-vector networks. *Mach Learn* 20(3):273–297
37. Schölkopf B, Burges C, Vapnik V (1995) Extracting support data for a given task. In: KDD
38. Mattern D, Haykin S (1999) Support vector machines for dynamic reconstruction of a chaotic system. In: Advances in kernel methods. MIT Press, Cambridge, pp 211–241
39. Smola AJ, Schölkopf B (2004) A tutorial on support vector regression. *Stat Comput* 14(3):199–222

40. Chang C-C, Lin C-J (2011) LIBSVM: a library for support vector machines. *ACM Trans Intell Syst Technol* 2(3):27
41. Knight D, Sellin R (1987) The SERC flood channel facility. *Water Environ J* 1(2):198–204
42. Blalock ME, Sturm TW (1981) Minimum specific energy in compound open channel. *J Hydraul Div* 107(6):699–717
43. Knight DW, Demetriou JD (1983) Flood plain and main channel flow interaction. *J Hydraul Eng* 109(8):1073–1092
44. Lambert M, Sellin R (1996) Discharge prediction in straight compound channels using the mixing length concept. *J Hydraul Res* 34(3):381–394
45. Lambert MF, Myers W (1998) Estimating the discharge capacity in straight compound channels. *Proc ICE-Water Marit Energy* 130(2):84–94
46. Bousmar D, Zech Y (1999) Momentum transfer for practical flow computation in compound channels. *J Hydraul Eng* 125(7):696–706
47. Haidera M, Valentine E (2002) A practical method for predicting the total discharge in mobile and rigid boundary compound channels. In: *International conference on fluvial hydraulics, Belgium*. pp 153–160
48. Bousmar D, Wilkin N, Jacquemart J-H, Zech Y (2004) Overbank flow in symmetrically narrowing floodplains. *J Hydraul Eng* 130(4):305–312
49. Knight D, Shiono K, Pirt J (1989) Prediction of depth mean velocity and discharge in natural rivers with overbank flow. In: *Proceedings of the international conference on hydraulic and environmental modelling of Coastal, Estuarine and River Waters*, pp 419–428
50. Tarrab L, Weber J (2004) Predicción del coeficiente de mezcla transversal en cauces aturales. *Mecánica Computacional, XXIII, Asociación Argentina de Mecánica Computacional, San Carlos de Bariloche*, pp 1343–1355
51. Brunner GW CEIWR-HEC (2010) HEC-RAS river analysis system user's manual version 4.1. In: *Tech. Rep., US Army Corps of Engineers Institute for Water Resources Hydrologic Engineering Center (HEC), CA, USA*